JOURNAL OF MATERIALS SCIENCE 28 (1993) 909–916

Creep behaviour of $Si_3N_4/Y_2O_3/Al_2O_3/AlN$ alloys

J. CRAMPON, R. DUCLOS, N. RAKOTOHARISOA
Laboratoire de Structure et Propriétés de l'état Solide, URA CNRS 234, Bât C6, Université des Sciences et Technologies de Lille 59655 Villeneuve d'Ascq Cedex, France

The compression creep behaviour of pressureless sintered $Y_2O_3/Al_2O_3/AlN$-doped Si_3N_4 was studied between 1473 and 1673 K, under stresses ranging from 100–300 MPa. Strain rate versus stress and temperature analysis give a stress exponent $n \simeq 1$ and an activation energy $Q = 860\ kJ\ mol^{-1}$. Microstructural change was investigated by transmission electron microscopy. The observed strain whorls, the stress exponent and the activation energy are indicative of a solution–diffusion–precipitation accommodated grain-boundary sliding where the diffusion through the glass is rate controlling.

1. Introduction

The need for advanced materials in certain structural applications at high temperature where low thermal expansion, low density and good oxidation resistance are required, has led to the development of high creep-strength Si_3N_4 produced primarily by hot pressing or sintering of ultra-fine powders. However, such a method does not allow a complex shape to be obtained and, due to the hardness of the fully dense Si_3N_4, diamond tool machining is normally required. An attractive alternative route for the fabrication of dense intricate components may be offered by electrical discharge machining. Indeed, it has been shown recently that Si_3N_4-based composites with suitable electrical conductivity can be obtained by adding a conductive second phase such as carbide or nitride particles [1–3].

Of course, for high-temperature technical applications, the composition of the composites must be adjusted in order to obtain the best compromise between a high creep-strength and a high level of electrical conductivity [2]. Si_3N_4-based ceramics with the best high-temperature properties may be fabricated today via pressureless sintering or hot isostatic pressing [4] using a liquid densification medium. It is now well established that these properties are strongly dependent upon the residual intergranular phases which can be either glassy or crystalline and which may be modified during post-sintering heat treatments [5–9]. In this respect, the $Y_2O_3/Al_2O_3/AlN$-doped Si_3N_4 seems to be an ideal matrix for electroconductive silicon nitride-based composites by adding TiN conductive particles. The improvement of the mechanical properties of the resulting composites needs at first the determination of the high-temperature deformation and microstructure characteristics of the Si_3N_4 matrix.

This paper reports the results of a microstructural and mechanical study of compressive creep of pressureless sintered $Y_2O_3/Al_2O_3/AlN$-doped Si_3N_4 matrix; the results for the composites are presented elsewhere [10]. In pressureless-sintered silicon nitride the deformation is strongly dependent on the viscosity of the grain-boundary glassy phase and the reactions across the glass/silicon nitride crystal interfaces. In a previous paper, it has been established that in the case of pressureless-sintered $MgAl_2O_4$-doped Si_3N_4 the transfer of atoms across the glassy/matrix interfaces appeared as the rate-controlling step of creep up to 1533 K and 200 MPa [11]. In the case of $Y_2O_3/Al_2O_3/AlN$-doped materials, the glassy phase may partially crystallize during post-sintering treatments giving either β'-Si_3N_4 + YAG or β'-Si_3N_4 + $Y_2Si_2O_7$ as dominant crystalline phases. Development microstructures of this type have been studied by Lewis *et al.* [9] including a bend and compressive creep study [12, 13]. The creep properties of pressureless-sintered Si_3N_4 ceramics with $Y_2O_3/Al_2O_3/AlN$ additions have initially been studied by Lumby *et al.* [14] ; viscous flow of the glassy phase or crystal plasticity in the crystallized material was suggested as the rate-controlling process accommodating sliding. After this preliminary work, Lewis *et al.* [12] studied the mechanisms of creep deformation in two-phase (β'-Si_3N_4 + YAG) microstructure. These materials obtained by post-sintering heat treatment, exhibit an apparent power-law creep in bend tests ($n = 4$) attributed to plasticity of the garnet phase. The activation energy for creep was found to be $Q = 900\ kJ\ mol^{-1}$. However, this high stress exponent was infirmed by compressive tests exhibiting values of $n = 2$. Following this study, Lewis *et al.* [13] reexamined the high-temperature creep of pressureless-sintered two-phase β'-Si_3N_4 ceramics and found that as-sintered ceramics exhibit a stress exponent $n = 1$ which has been interpreted as a "viscous" glassy-phase flow-controlled mechanism. The activation energy for precrystallized materials, of the same order as monophase grain-boundary diffusion values [12], was attributed to interface/grain-boundary diffusion (Coble creep [15]).

It is obvious from these studies that the identification of rate-controlling mechanisms for these materials is not yet well established. Moreover, a recent review of creep in Si_3N_4 [16] has concluded that elucidating the creep rate-controlling mechanism for these $Y_2O_3/Al_2O_3/AlN$-doped materials is not easy.

In the present case, compressive creep was studied on as-sintered materials in order to examine a situation which is not well documented. The isostructural stress exponent has been determined in the temperature range 1573–1643 K, giving a value near unity and suggesting, together with the observed strain whorls, a Newtonian viscous grain-boundary sliding. Moreover, from the value of the isostructural activation energy, $Q = 860\ kJ\ mol^{-1}$, it is shown that the diffusion of matter through the residual intergranular glassy phase, which is known to be more viscous than that of $MgAl_2O_4$-doped material, is the limiting one rather than the interface-reaction step.

2. Experimental procedure

2.1. Materials

The $Y_2O_3/Al_2O_3/AlN$-doped Si_3N_4 materials were supplied by Céramiques Techniques Desmarquest (CTD), Evreux, France. Billets were prepared from commercial Si_3N_4 powder to which Y_2O_3, Al_2O_3, and AlN of high-purity grade were added. Pressureless sintering following cold-pressing was then performed under a nitrogen atmosphere at about 2023 K [17].

2.2. Creep testing and observations

Specimens ($3 \times 3 \times 10\ mm^3$) were machined from billets in which a three-point bend strength study performed by CTD at room temperature indicated that rupture stress was 771 ± 66 MPa. Sample density, as determined by hydrostatic weighing in pure alcohol, was found to be 3.14 before creep and did not change significantly in unfractured crept specimens.

Compressive creep experiments were performed in air and in argon between 1473 and 1673 K, using a constant load equipment. Stresses ranging from 100–300 MPa were applied to the samples by Si_3N_4 push rods and SiC discs to prevent indentation. Total dimensional variation was measured by a high-temperature probe which activated a linear variable differential transformer (LVDT) with an accuracy within ± 2 μm. The deformed samples were cooled down under load and their final dimensions were used to determine the true strain.

Thin foils obtained by ion-beam milling and taken from as-sintered and tested samples, were observed by transmission electron microscopy (TEM) throughout this work.

3. Results

3.1. Creep experiments

The results of the compressive creep experiments performed in air on pressureless sintered specimens are presented in Fig. 1. All the material showed transient

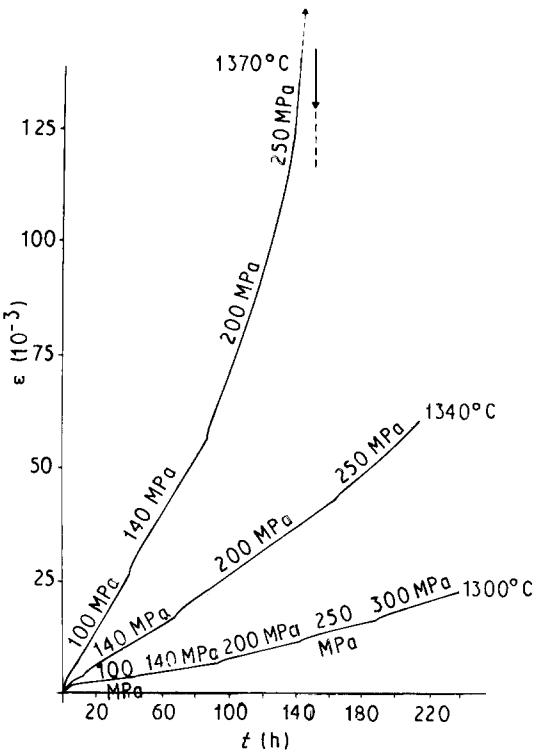

Figure 1 Creep curves ε–t (arrow indicates rupture of sample).

creep of about 5–10 h (primarily due to viscoelasticity) followed by a quasi steady-state region. A final tertiary period, with an acceleration of creep strain, was observed at the highest stresses and temperatures. Thus, acceleration of the creep begins to occur slowly under a stress of 250 MPa at 1613 K, and this acceleration leads quickly to the failure of the sample under the same stress at 1643 K.

The relationship between steady-state creep rate, stress and temperature was analysed with respect to the empirical law

$$\dot{\varepsilon}_s = A\sigma^n \exp - Q/kT \qquad (1)$$

where the coefficient A was dependent upon the microstructure (grain size, porosity, composition, . . .) of the sample. Owing to the possibility of a change in the microstructure during the highest temperature tests (by partial crystallization of the glassy phase, for example), the isostructural determinations of the stress exponent, n, and of the activation energy, Q, were made by the stress and temperature jump method. From the previous isothermal tests, which do not exhibit variations in creep stress exponent with time, the value of n was determined at each temperature and a mean value was found to be 0.9 ± 0.1 in air and in argon up to 1613 K for the whole stress range. At 1643 K in air a transition occurs at 200 MPa from a mean stress exponent of about 0.9 (140–200 MPa) to a value of about 2.4 (200–250 MPa).

Owing to a possible change of microstructure and composition with temperature, determination of the isostructural activation energy was made by decreasing and increasing temperature changes ranging between 1539 and 1673 K. A mean activation energy of about $860\ kJ\ mol^{-1}$, independent of time, was derived in air from tests ranging from 100–200 MPa.

3.2. Microstructural observations

In the transmission electron microscope, as-sintered Si_3N_4 generally appeared nearly dense, but the microstructure was rather inhomogeneous varying from about 0.25–1.2 μm in grain size for the equiaxed grains. The aspect ratio of the elongated grain, labelled A in Fig. 2, was greater than 6. The starting material showed a microstructure consisting of β-Si_3N_4 crystals embedded in a second phase which was highly electron absorbing and hence was always visible in darker contrast than the β-Si_3N_4 phase of low average atomic number. This second phase was generally a very localized glassy phase with sometimes small crystals of rounded shape inside the triple-junction pockets. In some cases, for the largest glassy pockets, the glassy nature of the phase could be detected in conventional area diffraction by a diffuse ring. The Si_3N_4 grains were primarily dislocation free, but few dislocations were visible inside the coarsest grains (2–3 μm).

After creep in air, transmission electron micrographs in the bulk of specimens show sometimes a microcrystallization of the glassy phase and often a crystallization of a semi-continuous second phase having a constant orientation over large areas and being highly absorbing in conventional diffraction contrast images. This is particularly visible for a sample submitted to increasing and decreasing temperature jumps of about 40 h each in the range 1473–1509–1539–1573–1613–1573–1539 K (Fig. 3). The identification of the intergranular phase structure made by electron diffraction patterns showed that the lattice had a garnet structure (centred cubic symmetry) with a lattice parameter 1.22 nm. This experimental parameter is compatible with that for yttrium–aluminium garnet (YAG) ($3Y_2O_3$–$5Al_2O_3$, lattice parameter 1.20 nm [18]) or eventually for a silicon-substituted form of "yttro-garnet" [9].

The partial devitrification of the glassy-phase occurred systematically during the creep tests for the whole

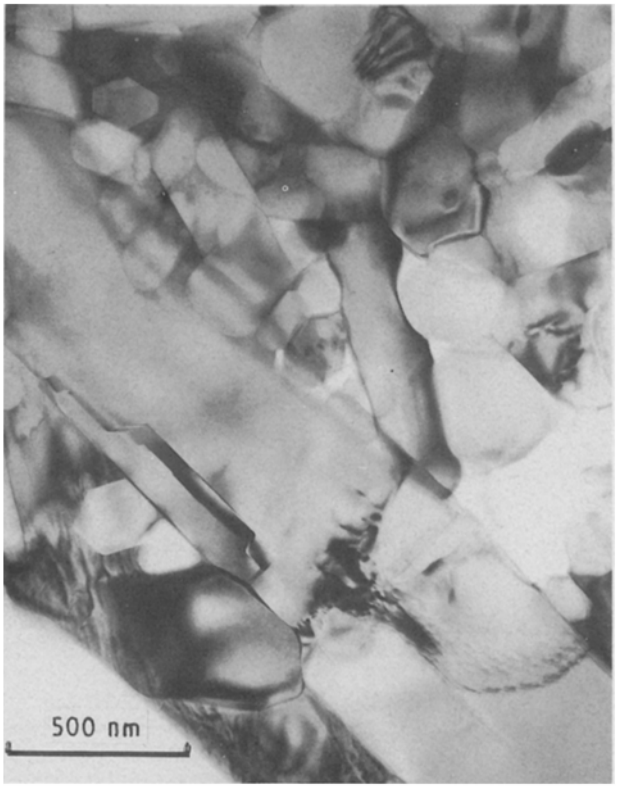

Figure 2 Transmission electron micrograph of an as-sintered Si_3N_4 sample.

Figure 3 Transmission electron micrographs of a crept sample: (a) microcrystallization, (b) bi-phased microstructure; $t = 218$ h; $T = 1473$–1613 K; $\sigma = 200$ MPa.

temperature range. Up to 1643 K the microstructure showed a dominant crystalline second phase formed by YAG grains, the size and the quantity of which depend upon the kind of thermal cycle applied to the sample. However, and in a rather marked manner, the samples which have been heated to 1673 K revealed yet larger glassy pockets.

In crept samples which were deformed at the highest temperatures (1643–1673 K) in the tertiary creep, damaged areas could be seen in the vitreous phase. As shown in Fig. 4, TEM revealed the appearance of round-shaped cavities which were formed and grew within the glassy phase. These cavities were never observed on reference samples and are therefore well related to the deformation. The mechanism of cavitation in tertiary creep seemed similar to other investigations [19–21] on cavitational deformation of Si_3N_4 and was not studied further.

The most distinctive deformation-induced feature found in crept and cooled-under-load samples was very numerous strain-fringes located along grain boundaries, as already observed in crept specimens of different Si_3N_4 alloys [5, 11, 22, 23]. These strain whorls, more numerous than in $Si_3N_4/MgAl_2O_4$ alloys, evidence the occurrence of grain-boundary sliding. It was determined that no asperities such as microprecipitates could be resolved in conventional TEM as being the origin of these whorls, but some whorls were found to be associated with a micro-stepped grain boundary (Fig. 5a).

3.3. Oxidation phenomenon

Crystalline-phase identification by X-ray diffraction patterns of as-sintered material confirmed the predominance of β-Si_3N_4 relative to α-Si_3N_4($\beta/(\beta + \alpha) \simeq 1$), and X-ray lines could also be matched with minor phases such as YAG [24].

After creep, external surfaces were covered with an oxide layer which was either glassy or crystalline

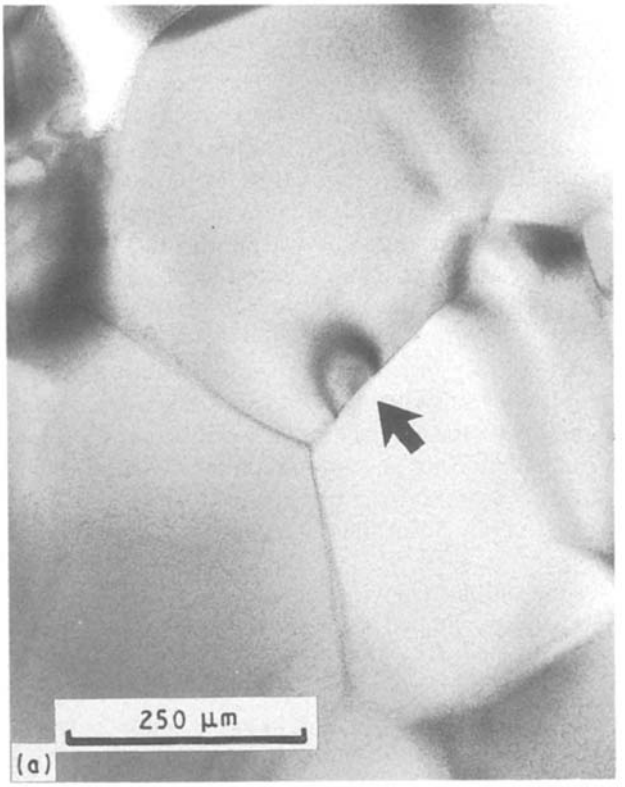

Figure 4 Transmission electron micrograph of a crept sample showing rounded cavities within the residual glassy phase; $t = 210$ h; $T = 1673$–1539 K; $\sigma = 140$ MPa.

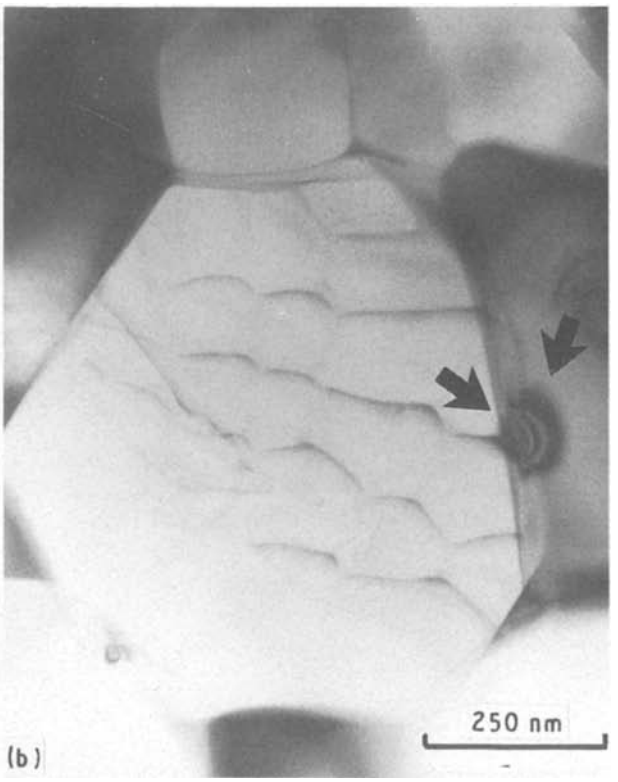

Figure 5 Transmission electron micrographs of crept samples showing strain whorls. (a) $t = 188$ h, $T = 1613$ K, $\sigma = 250$–200 MPa; (b) $t = 216$ h, $T = 1573$–1673 K, σ-140 MPa.

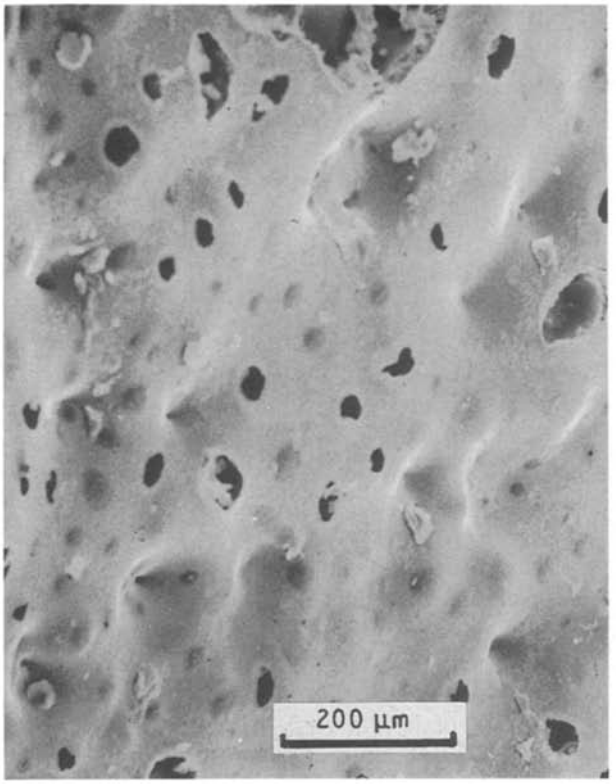

Figure 6 Scanning electron micrograph of the external surface of a crept sample showing the glassy external film: $t = 212$ h, $T = 1613$ K.

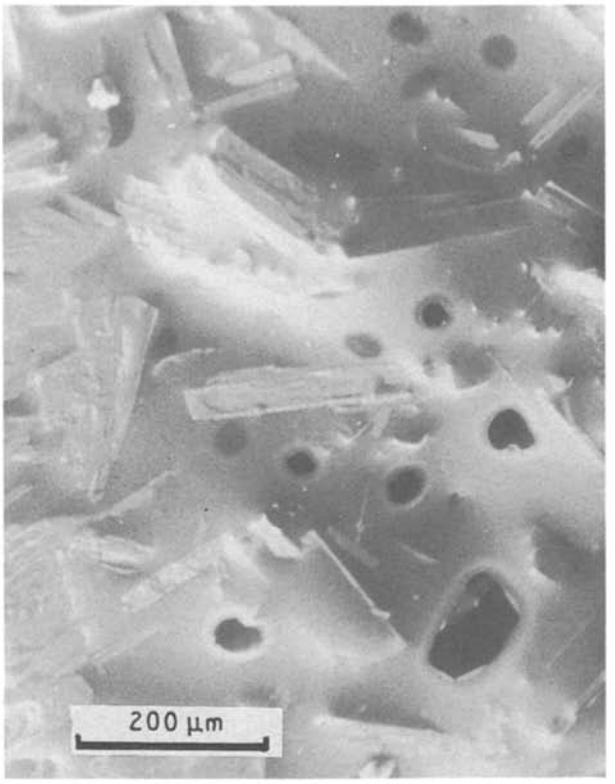

Figure 7 Scanning electron micrograph of the external surface of a crept sample showing acicular crystals embedded in a glassy film; $t = 153$ h, $T = 1643$ K.

according to the temperature, duration and cooling conditions of the test:

(a) for specimens creep tested more than 200 h at $T \geqslant 1573$ K (Fig. 6), a glassy external film the quantity of which increases at the highest temperatures, has been obtained. The holes and the bubbles in the glassy layer show the occurrence of gaseous nitrogen release;

(b) for relatively short time (100–150 h) of creep at $T \geqslant 1573$ K, a semi-crystalline external layer has been obtained. For example, a specimen creep tested 153 h at 1643 K (Fig. 7) was covered by acicular crystals embedded in a glassy oxide film. X-ray patterns of the external oxide film at room temperature revealed the crystallization of a small amount of yttrium disilicate (β-$Y_2Si_2O_7$), formed together with the vitreous film and very small quantities of cristobalite (α-SiO_2) and silicon oxynitride (Si_2N_2O).

Concentration profiles through cross-sections have been made for Al^{3+}, Y^{3+} and Si^{4+} by secondary ion mass spectroscopy (SIMS). The data were normalized with respect to silicon which showed a constant distribution over the whole depth of the samples. The analysis did not show clear evidence for the migration of Al^{3+}, but concentration profiles for Y^{3+} revealed a depletion of this ion in a narrow zone and a heterogeneous distribution, relative to the aluminium spectrum, in the specimen crept for 188 h at 1613 K (Fig. 8). The migration of yttrium towards the external surface was also observed during oxidation of a two-phase Si–Al–O–N (β'-Si_3N_4 + YAG) [25] and Bouarroudj *et al.* [26] reported segregation of yttrium to the subscale during oxidation of $70Si_3N_4$–$25SiO_2$–$5Y_2O_3$ (mol %).

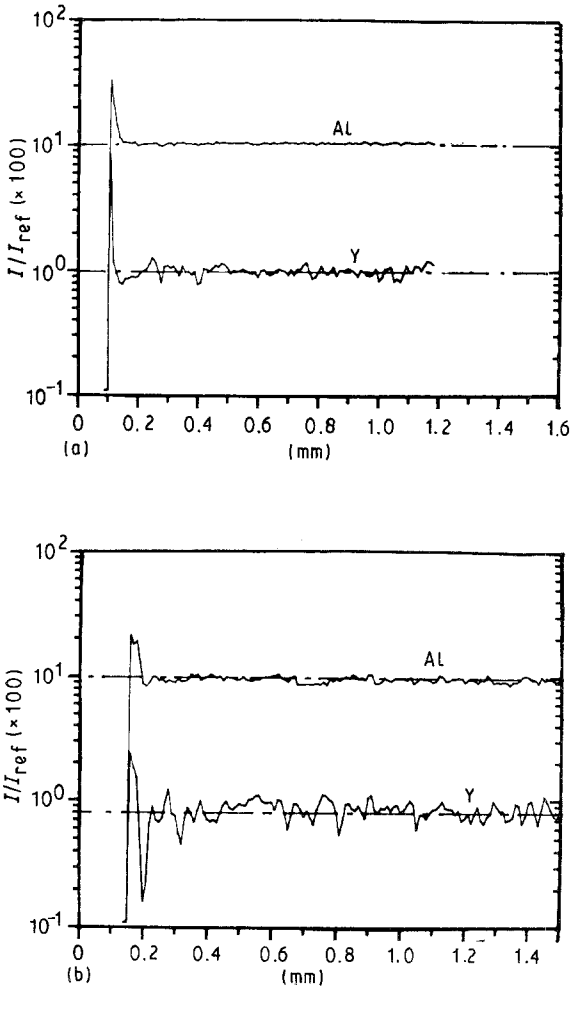

Figure 8 Concentration profiles for (a) reference sample, and (b) crept sample.

4. Discussion

4.1. Oxidation during creep

The addition of Y_2O_3, Al_2O_3 and AlN, for pressureless sintering of Si_3N_4 produced simultaneously solid solution of Al^{3+} and O^{2-} ions in the lattice of β-Si_3N_4 to form ceramic alloys of the following general composition: β'-$Si_{6-x}Al_xO_xN_{8-x}$ + Y–Si–Al–O–N glassy phase (here the maximum value of x is 0.29 [27]). Based on the Y–Si–O–N system, and neglecting for the moment the effect of aluminium and other possible cation impurities, our material has an approximate composition $86Si_3N_4$–$11SiO_2$–$3Y_2O_3$ (mol %), close to the Si_3N_4–Si_2N_2O tie line and far from the binary eutectics of the two other tie lines Si_2N_2O–$Y_2Si_2O_7$ and Si_3N_4–$Y_2Si_2O_7$ in the Si_3N_4–Si_2N_2O–$Y_2Si_2O_7$ compatibility triangle [28]. Furthermore, due to the small SiO_2/Y_2O_3 ratio in the starting composition, the formation of the J–H–K quaternary phases [28] has been greatly lowered and thus the so-called "catastrophic" oxidation has been avoided [24].

A parallel could be established between the oxidation during creep of our material and the oxidation of MgO-doped Si_3N_4 [29]. Schematically, passive oxidation of silicon nitride grains at high oxygen contents in the air produced a silica-rich layer at the surface. As a result, a chemical potential gradient was formed between this silica film and the glassy intergranular phase. This led to the outward diffusion of Y^{3+} cations within the original intergranular phase, their observed depletion in a zone narrow to the oxide layer/substrate interface and finally their extraction into the superficial oxide scale to form β-$Y_2Si_2O_7$ according to the reactions

$$2Y^{3+} + 3O^{2-} \rightarrow Y_2O_3 \quad (2)$$

$$Y_2O_3 + 2SiO_2 \rightarrow Y_2Si_2O_7 \quad (3)$$

A parallel flux of N^{3-} anions to the oxide scale should occur to ensure electrical neutrality and these ions are released as nitrogen gas, forming bubbles in the oxide film at the surface (Fig. 6).

For short-term oxidation ($t < 90$ h, $T = 1613$ K), all silica formed by passive oxidation has reacted with yttrium, and this has allowed the detection of the minor phase Si_2N_2O by XRD through the oxide scale. For long-term oxidation ($t > 370$ h, $T = 1613$ K) the outward flux of Y^{3+} decreases, either because crystalline phases (YAG) appear simultaneously with oxidation, or because a decrease in the composition gradient occurs as the equilibrium composition for the formation of β-$Y_2Si_2O_7$ proceeds. As the quantity of β-$Y_2Si_2O_7$ in the oxide scale was sufficient to form α-cristobalite nucleation sites, silica was present in the crystalline form, especially after decreasing temperature jump tests corresponding to a slow cooling rate. The glassy form of silica became preponderant for the longest and normally cooled creep tests.

This oxidation mechanism is in agreement with our observations of the surface morphologies and with those of Bouarroudj *et al.* [26] during oxidation of $70Si_3N_4$–$25SiO_2$–$5Y_2O_3$ (mol %). It was suggested that the diffusion through the glassy intergranular phase of a "yttrium–nitrogen" complex species should be the rate-controlling process.

4.2. Deformation mechanism during steady-state creep

The dominant creep mechanism of $Y_2O_3/Al_2O_3/AlN$-doped Si_3N_4 can be identified from the preceding experimental data and microstructural observations. The absence of dislocation activity within the grains proves the predominance of creep mechanisms other than dislocation creep. Similar conclusions have been drawn, for differently doped Si_3N_4, in previous investigations [5, 11, 19, 20].

The value near unity found for the stress exponent suggests that a viscous mechanism was prevailing in the present study. The presence of numerous strain whorls at the grain boundaries was the manifestation of grain-boundary sliding accommodated either by the elastic strain of the Si_3N_4 grains leading to the viscoelastic mechanism, or by some matter transport producing quasi-steady-state creep.

Depending on temperature, strain, stress, viscosity and concentration of the residual glassy phase, the grain-boundary sliding in silicon nitride can be accommodated either by pure diffusional creep, by viscous flow of the glassy phase, or by the dissolution–diffusion–reprecipitation of material. Although Coble creep [15], with a high activation energy of 800–900 kJ mol^{-1} has been put forward by Lewis *et al.* [13] in two-phase Si–Al–O–N (β'-Si_3N_4 + YAG), it is unlikely that pure diffusional creep processes would be rate-controlling in the presence of a residual glassy phase not completely recrystallized as in our case. Moreover, grain-boundary sliding controlled by the flowing transfer of the viscous phase from boundaries under compression to those in tension [30] can be also ruled out, because crystallization of the glassy phase occurring during creep has lowered its amount down to volume fractions which would not be sufficient to produce steady-state deformation as observed.

A stress exponent of 1, and strain whorls at highly stressed contact points between grains are thus evidence for a mechanism where grain-boundary sliding is accommodated by solution–diffusion–precipitation [31]. Stress concentrations have already been identified in earlier studies [5, 11] as a driving force for this mechanism in Si_3N_4.

The solution–diffusion–precipitation mechanism must be controlled by the slowest of two steps; either by the interface reaction or by the diffusion through the glassy phase. If the last is rate-controlling, then the activation energy for creep will depend on the viscosity of the glassy phase. The isostructural activation energy for steady state creep, found to be 860 kJ mol^{-1} in the present work, will now be compared with activation energies from other creep studies and oxidation kinetics where the diffusion through the glass was rate-controlling.

Creep studies of Y_2O_3-doped Si_3N_4, deformed in three or four-point flexure, give activation energy values ranging from 700–780 kJ mol^{-1} [8, 26, 32]. Bouarroudj *et al.* [26] found a stress exponent of 1, and they showed that the activation energy for the viscoelastic and the diffusional components of the primary creep was of the same value (720 kJ mol^{-1}).

By comparison of activation energy for creep with that for oxidation kinetics (680 kJ mol^{-1}) they concluded that the rate-controlling step of the solution–precipitation mechanism was the diffusion of a "yttrium–nitrogen" complex species through the glassy phase. Todd and Xu [32] found a stress exponent of 2 and an activation energy of about 700 kJ mol^{-1} in the $92Si_3N_4$–$6Y_2O_3$–$2Al_2O_3$ (wt %) composition, where the crystallization of the glassy phase in YAG was not reported. These results were consistent with a cavitational creep mechanism modelled by Evans and Rana [33]. From ionic radius consideration and from the analysis of Bouarroudj *et al.* [26], they concluded that the rate-controlling step was the nitrogen anion diffusion through the glassy phase.

The activation energy of the oxidation kinetics for the same material as in the present work ($[Y_2O_3/Al_2O_3]_{wt} = 2$) has been determined recently and was found to be 850 kJ mol^{-1} up to 1623 K for pressureless-sintered samples [34]. This value is very close to that measured here for the creep mechanism and to the activation energy value of 865 kJ mol^{-1} obtained for the oxidation kinetics below 1623 K in the $90Si_3N_4$–$6Y_2O_3$–$4Al_2O_3$ (wt %) system [35]. Thus, with regard to the microscopic process and not to the creep resistance due to the different amounts and composition of the glassy phase, the same deformation mechanism should be rate-controlling both for our $86Si_3N_4$–$11SiO_2$–$3Y_2O_3$ (mol %) material and for that of Bouarroudj *et al.* $70Si_3N_4$–$25SiO_2$–$5Y_2O_3$ (mol %) [26]. Support for the view that the diffusion through the glassy phase, rather than interface-reaction step, was rate-controlling can be taken from the study of Hamsphire and Jack [36] who have concluded that the kinetics of sintering of Y_2O_3-doped Si_3N_4 was also diffusion controlled. Moreover, it can be noted that our activation energy for creep falls in the activation energy range for the viscosity of Si–Y–Al–O–N glasses above T_g [37]. Finally, at this state of the existing diffusion data for silicon nitride, it seems rash to try to specify which microscopic species is the rate-limiting one.

5. Conclusions

1. Compression creep tests were made in the temperature range 1473–1673 K on pressureless sintered $Y_2O_3/Al_2O_3/AlN$-doped Si_3N_4, giving a stress exponent $n \approx 1$ and an activation energy $Q = 860$ kJ mol^{-1}.

2. The observed strain whorls, together with the stress exponent, can be discussed in terms of solution–diffusion–precipitation accommodated grain-boundary sliding.

3. The activation energy is in agreement to that obtained for the oxidation kinetics on the same material and on the $90Si_3N_4$–$6Y_2O_3$–$4Al_2O_3$ (wt %) system below 1623 K, and falls in the activation energy range for the viscosity of Si–Y–Al–O–N glasses above T_g.

4. These results, together with the analysis of Bouarroudj *et al.*, support the view that the diffusion through the glass, rather than the transfer of atoms across the glass/crystal interface, is rate-controlling.

Acknowledgements

The authors thank Dr B. Cales and colleagues, C. T. Desmarquest, Evreux, France, for help in producing the Si_3N_4 billets, and Drs P. Eveno and M. Schumacher for performing the SIMS analysis. This work was supported by the French Research and Technology Ministry (MRT).

References

1. E. KAMIJO, M. HONDA, M. HIGUCHI, H. TACKEUCHI and T. TANIMURA, *Sumitomo. Elec. Tech. Rev.* **24** (1985), 183.
2. C. MARTIN, B. CALES, P. VIVIER and P. MATHIEU, *Mater. Sci. Engng A* **109** (1989) 351.
3. A. BELLOSI, A. FIEGNA and G. N. BABINI, in "Euro-Ceramics 3", Proc ECerS '89, edited by G. de With, R. A. Terpstre, R. Metselaar (Elsevier Applied Science, London, 1989) pp. 389–93.
4. J. C. MARTIN, H. TAKATA and K. ISHIZAKI, *J. Ceram. Soc. Jpn Inter.* **96** (1988) 874.
5. F. F. LANGE, B. T. DAVIS and D. R. CLARKE, *J. Mater. Sci.* **15** (1980) 601.
6. D. R. CLARKE, F. F. LANGE and G. D. SCHNITTGRUND, *J. Amer. Ceram. Soc.* **65** (1982) C 51.
7. D. R. CLARKE, *J. Amer. Ceram. Soc.* **66** (1983) 92.
8. T. CHARTIER, J. L. BESSON, P. COURSAT and W. MUSTEL, *J. Phys.* **47** (1986) C1-673.
9. M. H. LEWIS, A. R. BHATTI, J. R. LUMBY and B. NORTH, *J. Mater. Sci.* **15** (1980) 103.
10. J. CRAMPON, R. DUCLOS, *Acta Metall. Mater.* **38** (1990) 805.
11. J. CRAMPON, R. DUCLOS and N. RAKOTOHARISOA, *J. Mater. Sci.* **25** (1990) 1203.
12. M. H. LEWIS, B. S. B. KARUTARATNE, J. MEREDITH and C. PICKERING, "Creep and Fracture of Engineering Materials and Structures, Proceedings of an International Conference, University College", Swansea, edited by B. Wilshire and D. R. J. Owen (1981) 365–79.
13. M. H. LEWIS, G. R. HEATH, S. M. WINDER and R. J. LUMBY, in "Deformation of Ceramic Materials II", edited by R. E. Tressler and R. C. Bradt, Vol. 18 (1984) pp. 605–16.
14. R. J. LUMBY, B. NORTH and A. J. TAYLOR, Army Materials and Mechanics Research Center, "Procedings of the 5th Materials Technology Conference", Newport, RI (1977).
15. R. L. COBLE, *J. Appl. Phys.* **34** (1963) 1679.
16. C. da SILVA and T. J. DAVIES, in "Creep and Fracture of Engineering Materials and Structures", Proceedings of the International Conference University College Swansea, edited by B. Wilshire and R. W. Evans (1987) pp. 989–1005.
17. J. P. TORRE and Y. BIGAY, *Ceram. Engng Sci.* **7** (1986) 893.
18. M. L. KEITH and R. ROY, *Amer. Mineral.* **39** (1984) 1.
19. R. KOSSOWSKY, D. G. MILLER and R.S. DIAZ, *J. Mater. Sci.* **10** (1975) 983.
20. S. U. DIN and P. S. NICHOLSON, *ibid.* **10** (1975) 1375.
21. J. M. BIRCH and B. WILSHIRE *ibid.* **13** (1978) 2627.
22. J. CRAMPON, R. DUCLOS, N. RAKOTOHARISOA, Y. BIGAY, B. CALES and J. P. TORRE, in "S.C.14", edited by D. Taylor (The Institute of Ceramics, Stock on Trent, UK, 1988) p. 575.
23. G. D. QUINN and W. R. BRAUE, *J. Mater. Sci.* **25** (1990) 4377.
24. L. THEMELIN, Doctoral thesis, University of Limoges, France, November 1989.
25. M. H. LEWIS and P. BARNARD, *J. Mater. Sci.* **15** (1980) 443.
26. A. BOUARROUDJ, P. GOURSAT and J. L. BESSON, *ibid.* **20** (1985) 1150.
27. N. S. RAKOTOHARISOA, Ing. Doct. thesis, USTLFA, Villeneuve d'Ascq. France, November 1988.
28. L. J. GAUCKLER, H. HOHNKE and T. Y. TIEN, *Bull. Amer. Ceram. Soc.* **57** (1978) 828.
29. D. R. CLARKE and F. F. LANGE, *J. Amer. Ceram. Soc.* **63** (1980) 586.

30. M. H. LEWIS, B. D. POWELL, P. DREW, R. J. LUMBY, B. NORTH and A. J. TAYLOR, *J. Mater. Sci.* **12** (1977) 61.
31. R. RAJ and C. K. CHYNG, *Acta Metall.* **29** (1981) 159.
32. J. A. TODD and Z. Y. XU, *J. Mater. Sci.* **24** (1989) 4443.
33. A. G. EVANS and A. RANA, *ibid.* **28** (1980) 129.
34. L. THEMELIN, M. DESMAISON, J. CRAMPON, M. BILLY and B. CALES, *Ceram. Inter.*, to be published.
35. J. ECKEBERRIA and F. CASTRO, in "Euro-Ceramics 3" Proc ECerS '89, edited by G. de With, R. A. Terpstra and R. Metselaar (Elsevier Applied Science, London, 1989) pp. 527–32.
36. S. HAMSPHIRE and K. H. JACK, *Prog. Nitrogen Ceram.* **32** (1983) 225.
37. T. ROUXEL, J. L. BESSON and C. GAULT, in "Euro-Ceramics 3" Proc. ECerS '89, edited by G. de With, R. A. Terpstra and R. Metselaar (Elsevier Applied Science, London, 1989) pp. 351–5.

Received 12 April 1991
and accepted 1 May 1992